



NUMERICAL STUDY OF HEAT TRANSFER DUE TO TWINJETS IMPINGEMENT ONTO AN ISOTHERMAL MOVING PLATE

Anıl Başaran and Fatih Selimefendigil

Department of Mechanical Engineering, Celal Bayar University, 45140, Muradiye,
Manisa, Turkey
anil.basaran@cbu.edu.tr

Abstract-In this study, heat transfer from a moving isothermal hot plate due to double impinging vertical slot jets was investigated for a laminar flow. The rectangular geometry consists of a confining adiabatic wall placed parallel to the moving impingement. The jets are located symmetrically at mid point of upper wall. Water and Al_2O_3 nanoparticles mixture with different volumetric fraction was used as working medium. In considered jet impingement problem, the effects of the jet exit Reynolds numbers, ranging from 50 to 200, the normalized plate velocity, ranging from 0 to 2, and volumetric fractions of nanofluid, ranging from 0% to 6% were investigated. The commercial software package based on finite volume method FLUENT (version 6.3.26) is used in this study for the computations. It has been observed that increasing normalized plate velocity increases the heat transfer from bottom surface. Similarly, increasing Reynolds number of slot jets leads to enhancement of heat transfer. Besides, increasing volumetric fraction of nanofluid contributes to heat transfer enhancement.

Key Words- Jet flow, CFD, Nanofluid

1. INTRODUCTION

The impingement cooling found its use in early 1960's, especially in the high heat flux region such as in the gas turbine blade [1]. It received considerable attention due to its inherent characteristics of high heat transfer rate. Impinging jets find a vast amount of industrial application areas such as thermal treatment of surfaces, drying of textiles and papers, annealing of glass, cooling of electronic devices, turbine blades and outer walls of combustors. A jet of fluid from a slot or a circular hole is directed towards a targeted surface. High values of the local heat and mass transfer coefficients can be obtained with impinging jets. The advantage of impinging jet flow is its ease to adjust the location of interest and to remove a large amount of heat (or mass) on the impinging surface due to the thin hydrodynamic and thermal (or concentration) boundary layers around the stagnation region. In recent years, the power dissipation from electrical components becomes larger because of their high density. The impinging jet is used as a promising candidate to remove more heat from electrical components [2]. The nozzle geometry of impinging jets can be rectangular or circular. According to many studies conducted on impinging jets for circular and slot jets, the flow field and thermal characteristics are different in slot jets compared to circular jets. Jet flows can be classified according to their jet number in construction such as single, double or multiple jets [3].

Most of the studies reported parametric influence on the local heat transfer coefficient or method to enhance the heat transfer. Detailed topics included the effects of Reynolds number, nozzle configuration, turbulent intensity and target spacing [4]. The heat transfer analysis of impingement jets are considerably complicated due to flow recirculation, pressure gradients and local thinning of the boundary layer on the impingement surface.

A theoretical investigation of impingement heat transfer with single phase free slot jet was carried out by Chen et al. [5]. They divided the thermal and velocity boundary layer into four regions of flow from which they obtained correlations for the heat transfer coefficients.

Numerical studies of impinging jets were carried out by many researchers. Lou et al. [6] have carried out a numerical investigation to examine the effects of geometric parameters on confined impinging jet heat transfer. They noted that with the decrease of nozzle width and nozzle-to-plate spacing, heat transfer coefficient decreases and surface roughness generally deteriorates laminar impinging jet heat transfer. Sharif and Banerjee [7] have numerically made an analysis of heat transfer due to confined slot-jet impingement on a moving plate. They studied the effects of jet exit Reynolds number, normalized plate velocity and distance of separation between the impingement plate. They noted that the average Nusselt number increases considerably with the jet exit Reynolds number as well as with the plate velocity.

It can be seen from previously made related studies that researchers investigated not only single impinging jet but also double or multiple impinging jets. Hewakandamby [8] have studied heat transfer performance of double oscillatory impinging jets. The author developed a two-dimensional model using finite volume method to investigate the heat transfer performance with respect to the oscillation frequency, geometric parameters and the Reynolds number. Dagtekin and Oztop [3] have conducted a numerical study to investigate the heat transfer due to double laminar slot jets impingement onto an isothermal wall within closed long duct. They investigated the effects of the jet Reynolds number, the jet-isothermal bottom wall spacing, and the distance between two jets on heat transfer and flow field. They chose the air as working fluid in their study. They observed that the heat transfer is enhanced significantly when Reynolds number of the first jet is higher than second one.

In heat transfer applications, nano-sized particles (average particle size less than 100 nm) are added in the base fluid such as water or ethylene glycol to obtain better thermal properties compared to base flow. Nano fluids have improved heat transfer characteristics with little pressure drop as compared to base fluids [9]. The study of nanofluids in impinging jets have been conducted by many researchers [10]

In this study, the rectangular geometry both left and right are open and consist of a confining adiabatic wall placed parallel to the moving bottom plate was used as flow domain. Heat transfer from isothermal moving bottom plate due to double impinging vertical slot jets which symmetrically located in the mid-point of adiabatic upper confining wall was investigated numerically for laminar flow regime. The aim of the present study is to examine the effects of Reynolds number, nanoparticle volume fraction and normalized bottom plate velocity on heat transfer.

2. NUMERICAL SIMULATION

2.1. Description of flow domain

The rectangular flow domain is given in Fig 1. To simulate the confined nano-fluid array of jets impingement system some geometrical parameter and normalized plate velocity are shown in the figure. The two-dimensional flow domain considered in this study consist of a hot plate moving isothermal impingement plate of length L at the bottom, which is confined by a parallel adiabatic wall on top separated by a distance H from the impingement plate. The bottom plate is kept at temperature $T=T_h$. Here, L is long enough to satisfy fully developed flow in the duct. The slot-jets placed a distance of $2W$ from the middle of top surface wall. The jet from the slots on the top plate impinges on the bottom plate. The coordinate system is fixed in the middle of hot bottom moving wall. The normalized length of the domain (L/W) is kept fixed at 50 (extending from -25 to 25). Similarly, the normalized height of the domain (H/W) is at kept fixed at 6.

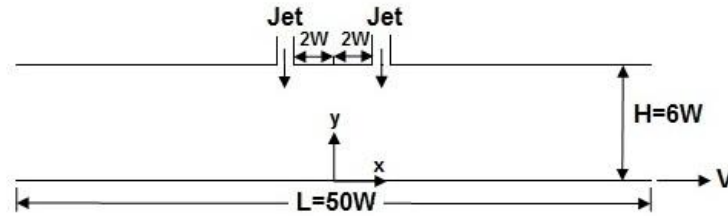


Figure 1. Schematics of the flow domain

2.2. Governing equations

In this configuration, the flow is 2D, laminar, incompressible and the fluid (nanofluid) physical properties (density, viscosity and thermal conductivity) are constant. With these assumptions, the mass, momentum, and energy conservation equations for the steady incompressible flow, neglecting the viscous dissipation, are given as follows

$$\frac{\partial u}{\partial x} + \frac{\partial v}{\partial y} = 0 \quad (1)$$

$$\rho \left(u \frac{\partial u}{\partial x} + v \frac{\partial u}{\partial y} \right) = -\frac{\partial p}{\partial x} + \mu \left(\frac{\partial^2 u}{\partial x^2} + \frac{\partial^2 v}{\partial y^2} \right) \quad (2)$$

$$\rho \left(u \frac{\partial v}{\partial x} + v \frac{\partial v}{\partial y} \right) = -\frac{\partial p}{\partial y} + \mu \left(\frac{\partial^2 u}{\partial x^2} + \frac{\partial^2 v}{\partial y^2} \right) \quad (3)$$

$$\rho c_p \left(u \frac{\partial T}{\partial x} + v \frac{\partial T}{\partial y} \right) = k \left(\frac{\partial^2 T}{\partial x^2} + \frac{\partial^2 T}{\partial y^2} \right) \quad (4)$$

where u , v , T and p represent the two velocity components, temperature and pressure, respectively. ρ , c_p , μ and k denote the density, specific heat, viscosity and thermal conductivity of nanofluid, respectively.

Local Nusselt number based on h and slot width W is defined as

$$Nu(x) = -\frac{hW}{k} \quad (5)$$

The scaling parameters are chosen as the average velocity at the jet V_0 ($=V_1+V_2$), the hydraulic diameter of jets w ($=w_1+w_2$). V_1 and V_2 are first and second jet velocity, respectively. w_1 and w_2 , first and second slot width. Therefore, hydraulic diameter of jet w becomes equal to $2W$.

In this respect, Reynolds number can be written as follows,

$$Re = \frac{(V_1 + V_2)2W}{\nu} \quad (6)$$

where ν is kinematic viscosity.

2.3. Boundary conditions

The boundary conditions for the considered problem in dimensional form can be written as

- At the ducts exit: $P = P_{atm}$
- At the bottom moving isothermal wall: $u = U_0; \quad v = 0; \quad T = 310K$
- At the adiabatic top wall: $u = 0; \quad v = 0; \quad \frac{dT}{dy} = 0$
- At the jet exits: $u = 0; \quad v = V_0$

2.4. Thermo-physical properties of the Al_2O_3 -water nanofluid

In the present study, water with Al_2O_3 nanoparticles is used as working fluid. The presence of nanoparticles alters the binary mixture properties. The following equations are used to compute thermo-physical properties of nanofluid (density, specific heat, viscosity and thermal conductivity) [11].

$$\rho_{nf} = (1-\phi)\rho_{bf} + \phi\rho_p \quad (9)$$

$$(c_p)_{nf} = (1-\phi)(c_p)_{bf} + \phi(c_p)_p \quad (10)$$

where the subscripts bf, nf and p denote the base fluid, nanofluid and nanoparticle volume fraction, respectively. Dynamic viscosity of the nanofluid is computed using the correlation obtained from the least squares curve fitting of the experimental data as Wang et al. [12]

$$\mu_{nf} = \mu_{bf}(123\phi^2 + 7.3\phi + 1) \quad (11)$$

Thermal conductivity of the nanofluid is obtained using the well known Hamilton and Crosser model (Hamilton and Crosser [13]) as,

$$k_{nf} = k_{bf}(4.97\phi^2 + 2.72\phi + 1) \quad (12)$$

Thermophysical properties of water and Al_2O_3 are given in Table 1.

Table 1. Thermophysical properties of water and Al₂O₃

	ρ (kg/m ³)	C _p (J/kgK)	k (W/mK)	μ (Pa.s)
Al ₂ O ₃	3380.0	773	36	
water	998.2	4182	0.5970	0.000998

2.5. Numerical Method

In this study, a finite volume method has been used to solve the governing equations. Eqs. (1) - (4) along with the boundary conditions and initial conditions are solved with the commercial software package FLUENT (version 6.3.26) from Fluent, Inc [14]. The convection terms has been discretized using the first-order upwind scheme while the diffusion terms are discretized using the central difference scheme. The SIMPLE algorithm has been used to couple the pressure and velocity. Convergence of the iterative solution has been insured when the residual of all the variables is less than the specified values. The specified values are convergence criteria are 10^{-3} for continuity, 10^{-5} for momentum, and 10^{-6} for energy. The computational domain consists of 19400 rectangular elements. The mesh independence of the solution has been assured.

3. RESULTS AND DISCUSSION

In this study, the rectangular flow domain with uniform grid distribution and given in Fig.1 was considered. The two-dimensional flow domain has two plates separated with distance H and length L. Double jets from vertical slots placed at adiabatic top plate impinges on the isothermal adiabatic moving bottom plate. The bottom plate is kept at temperature T=310 K. The normalized height of flow domain (H/W) is kept at 50 (ranging from -25 to 25) while the normalized length of flow domain (L/W) kept at 8. The bottom plate moves with a normalized velocity V towards right. Normalized velocity V is varied at discrete values of 0, 0.5, 1 and 2. Here, V=0 represents stationary bottom impingement plate.

Al₂O₃-water nanofluid with different nanoparticle volume fractions ϕ was selected as working fluid. Nanoparticle volume fractions ϕ are varied at values of 1%, 3%, 4% and 6%. Calculated thermo-physical properties of nanofluid accordingly Eqn 9-12 are given in Table 2.

Table 2. Thermo-physical properties of nanofluid for various volume fraction

	ρ (kg/m ³)	C _p (J/kgK)	K (W/mK)	μ (Pa.s)
ϕ (1%)	1022.0	4148	0.6135	0.001083
ϕ (3%)	1069.7	4080	0.6484	0.001327
ϕ (4%)	1093.5	4046	0.6667	0.001486
ϕ (6%)	1141.1	3977	0.7051	0.001877

In order to examine the effect of different Reynolds number on heat transfer a new parameter R was defined. R is ratio of jet Reynolds numbers and equal to $R=Re_2/Re_1$. Here, Re_1 and Re_2 are first and second jets Reynolds numbers, respectively.

As stated earlier, the main purpose of this study is to investigate the effects of laminar range of Reynolds number, between from 50 to 200, normalized plate velocity, ranging from 0 to 2, and nanoparticle volume fraction, ranging from 0% to 6% on heat transfer. In this respect, computations were carried out for total of 180 combinations of these parameters.

The isotherms for varying normalized plate velocity ($V=0$, $V=0.5$, $V=1$ and $V=2$) with $\phi=3\%$ and $Re_2=50$, $Re_1=50$ ($R=1$) are presented in Fig.2. It is shown in Fig.2 that with increase of normalized plate velocity thermal boundary layer becomes thinner resulting in increment of the temperature gradient. This means that there is an enhancement of heat transfer with increase of normalized plate velocity.

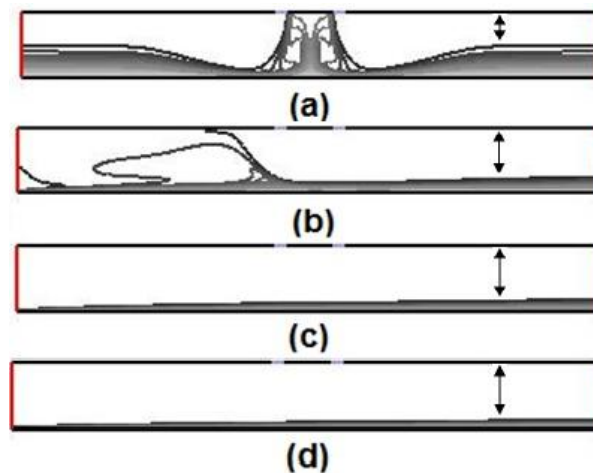


Figure 2. Isotherms for $\phi=3\%$, $Re_2=50$, $Re_1=50$ ($R=1$) (a) $V=0$ (b) $V=0.5$ (c) $V=1$ (d) $V=2$

The streamlines for varying normalized plate velocity ($V=0$, $V=0.5$, $V=1$ and $V=2$) with $\phi=3\%$ and $Re_2=50$, $Re_1=50$ ($R=1$) are given in Fig.3. According to Fig.3, after the jet impinges on the hot bottom, the flow is divided into both left and right side. For stationary plate case, three recirculation cells are formed whereas four recirculation cells are generated for the moving plate cases. When the bottom plate start to move the recirculation cells on the right are distorted and skewed to the right. The intensity of these recirculation cell decreases with increasing plate velocity.

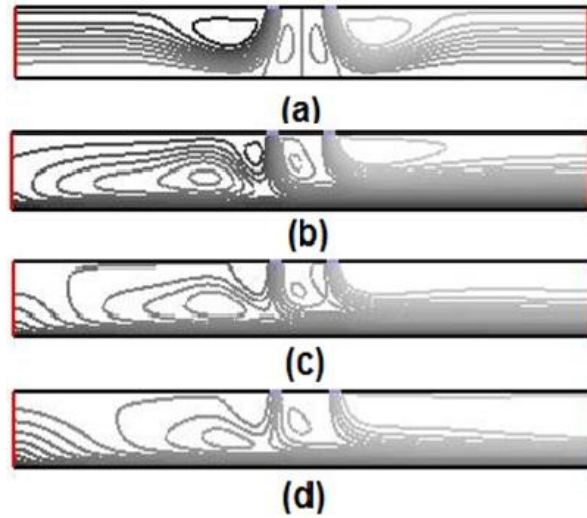


Figure 3. Streamlines for $\phi = 3$, $Re_2 = 50$, $Re_1 = 50$ ($R = 1$) (a) $V = 0$ (b) $V = 0.5$ (c) $V = 1$ (d) $V = 2$

Variation of the local Nusselt number along the impingement plate for various plate velocity at $\phi = 3$ and Reynolds number ratio $R = 0.5$, $R = 1$ and $R = 2$ is shown in Fig.4. It can be seen from the figure that peak values in the Nusselt number are obtained at stagnation point for the stationary plate case. As normalized plate velocity increase, peak values in the Nusselt number are obtained at the exit (ends of the impingement plate) and its value decrease along the impingement plate. For low plate velocity ($V = 0.5$) and low Reynolds number ratio ($R = 0.5$ [$Re_1 > Re_2$]) the shear driven effects by moving of plate are not important and distinct stagnation point is generated on the moving plate (Fig.4.a). On the other hand, for $R = 1$ ($Re_1 = Re_2$) and $R = 2$ ($Re_1 < Re_2$), distinct overshoot of local Nusselt number is not formed near the impingement point.

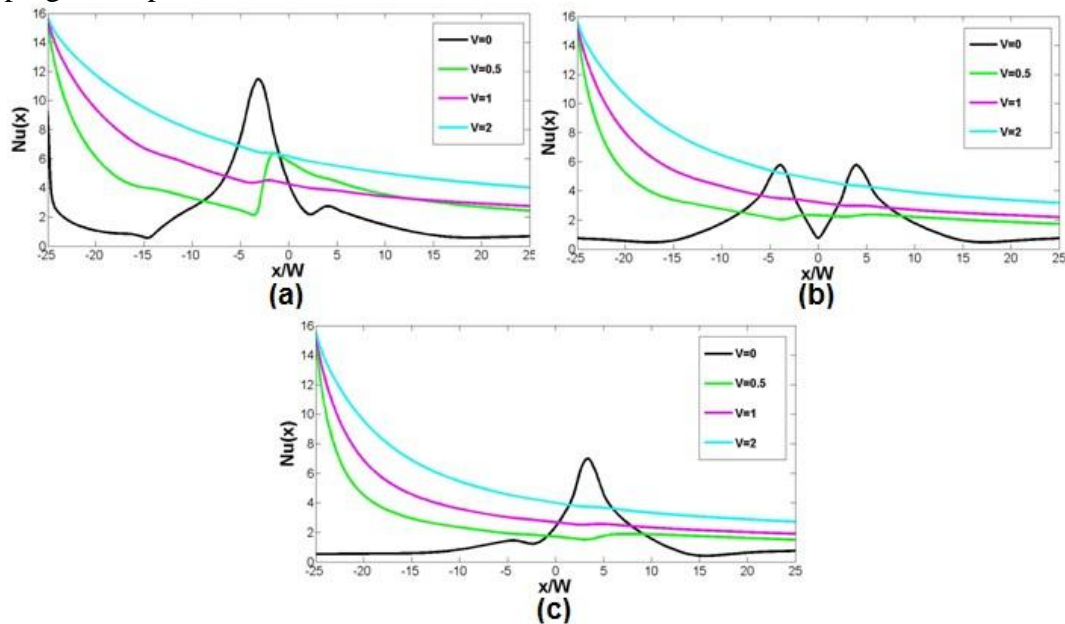


Figure 4. Variation of local Nusselt number various plate velocity for $\phi = 3$ (a) $R = 0.5$ (b) $R = 1$ (c) $R = 2$

In order to examine the effect of jet Reynolds numbers, the case of $\phi = 3$ and $V=1$ was considered. The isotherms for $\phi = 3$, $V=1$ and different Reynolds numbers are given in Fig.5 and Fig.6. Fig.5 shows the case that first jet Reynolds number is equal and higher than second jet Reynolds number, Fig.6 shows the case that first jet Reynolds number is equal and smaller than second jet Reynolds number. It can be seen from the figures that thermal boundary layer becomes thinner with increasing Reynolds number no matter which jet Reynolds number is higher. This results in enhancement of heat transfer.

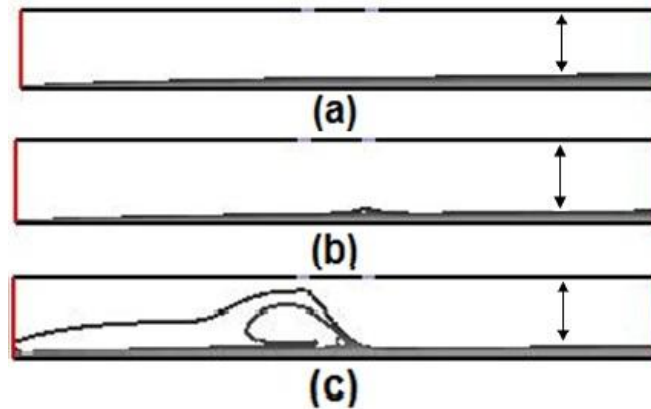


Figure 5. Isotherms for $\phi = 3$, $V=1$ (a) $Re_1=50$, $Re_2=50$ (b) $Re_1=50$, $Re_2=100$ (c) $Re_1=50$, $Re_2=200$

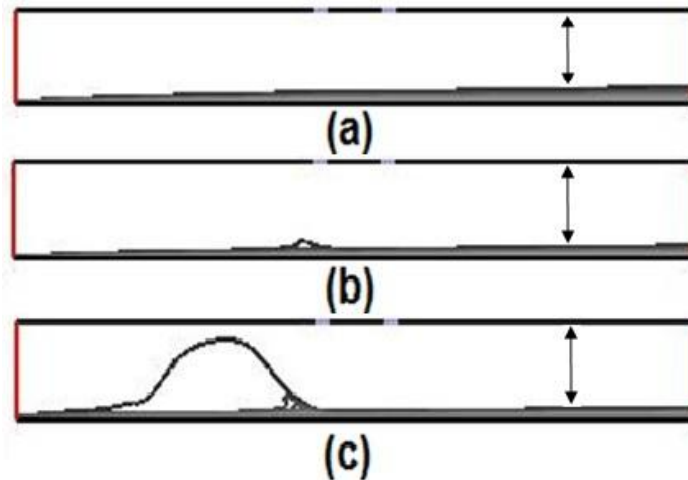


Figure 6. Isotherms for $\phi = 3$, $V=1$ (a) $Re_1=50$, $Re_2=50$ (b) $Re_1=100$, $Re_2=50$ (c) $Re_1=200$, $Re_2=50$

Fig.7 shows the streamlines for $\phi = 3$, $V=1$ at various Reynolds numbers. It is observed from the Fig.7 that as the jets impinge on the hot bottom surface three vortices are formed because of jets entrainment and confining effects of the top adiabatic wall. The vortices on the right are distorted and skewed to right and their intensity increase due to the increment of second jet Reynolds number. Similarly, intensity of vortices between the jets and on the left increase. Center of the vortices on the left also shift to the right with effect of powerful flow coming from second jet. According to Fig.7, the movement of bottom hot plate rather affects the flow at low jet velocity ($Re_1=50$, $Re_2=50$). In this case, the flows from first and second jets move in

direction of movement of bottom plate. The effect of movement of bottom plate on flow decrease with increasing second jet Reynolds number (Fig. 7.b and Fig. 7.c).

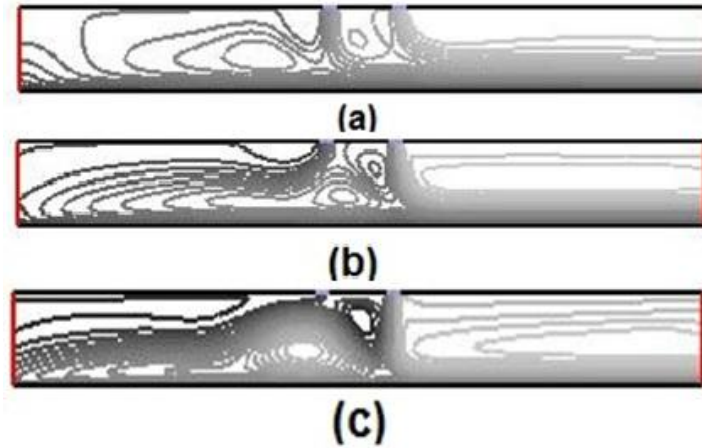


Figure 7. Streamlines for $\phi = 3\%$, $V = 1$ (a) $Re_1 = 50$, $Re_2 = 50$ (b) $Re_1 = 50$, $Re_2 = 100$ (c) $Re_1 = 50$, $Re_2 = 200$

Fig.8 shows the local Nusselt number distribution along the hot moving bottom impingement plate at various Reynolds number ratios 0.25, 0.5, 1, 2 and 4. Accordingly Fig.9, the peak value in the Nusselt number increases with adding nanoparticles. There is an increment in the local Nusselt number along the bottom plate in connection with increasing volume fraction. It is also possible to observe from Fig.11 that peak values in the Nusselt number are obtained at the exit similarly Variation of the local Nusselt number along the impingement plate for various plate velocity at $\phi = 3\%$ and Reynolds number ratio $R = 0.5$, $R = 1$ and $R = 2$. As one can see, with increasing volume fraction, heat transfer enhancement is obtained.

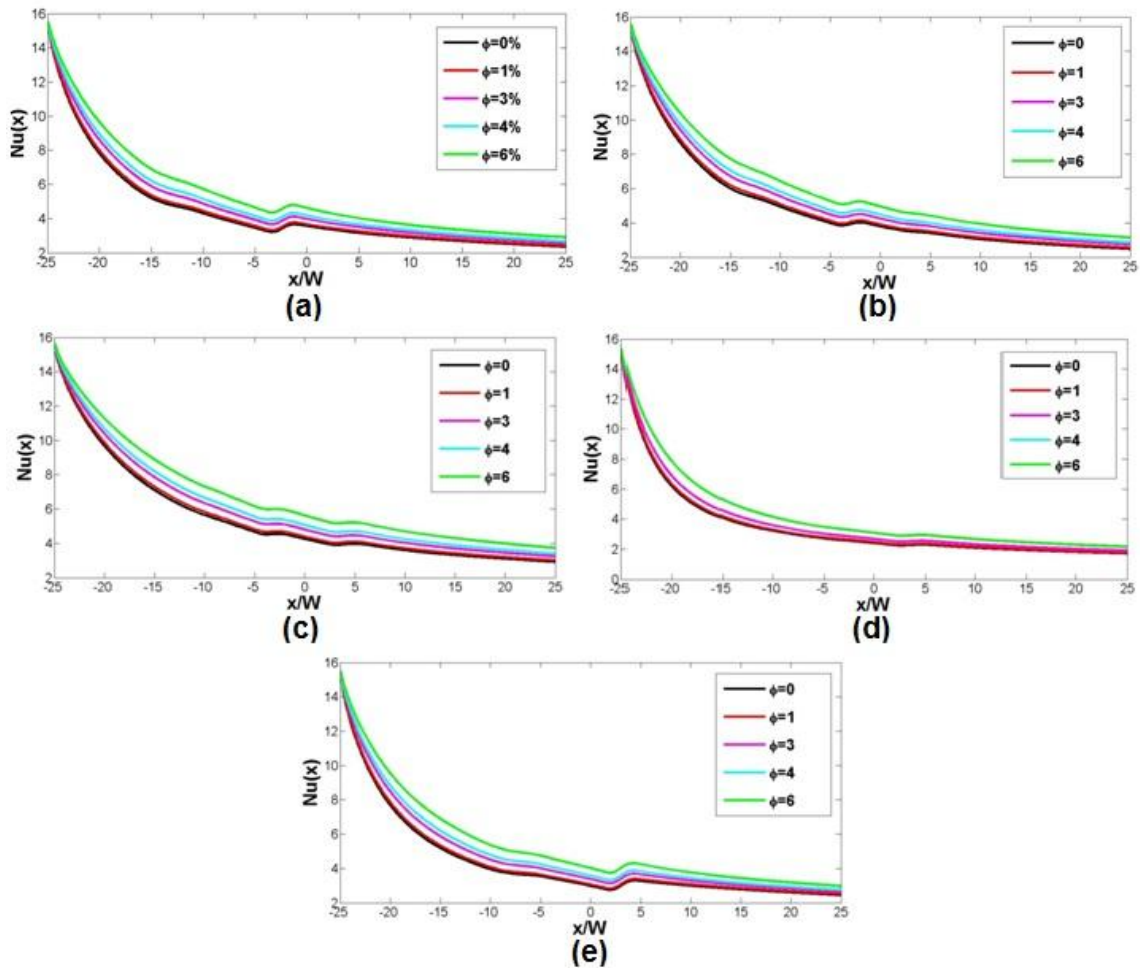


Figure 8. Variation of local Nusselt number along the hot bottom plate at various volume fraction for Reynolds number ratio (a) $R=0.25$, (b) $R=0.5$, (c) $R=1$, (d) $R=2$, (e) $R=4$.

4. CONCLUSION

In the current study, numerical investigation of heat transfer from a moving isothermal hot plate because of double impinging vertical slot jets is performed for different normalized plate velocity, Reynolds number and particle volume fraction. Following results are obtained:

- The plate velocity has significant effect on the flow and heat transfer in the flow domain. When the bottom hot plate velocity increases shear driven affects the flow domain. The peak value in Nusselt number is obtained near the impingement regions for stationary case whereas it is obtained at the exit for the moving plate case. The Nusselt number increase with increasing plate velocity.
- The Reynolds number also affects the flow domain and heat transfer process. The thermal boundary layer becomes thinner with increasing Reynolds number which results in enhancement of heat transfer

- The Nusselt number increases because of the adding nanoparticles. Heat transfer enhancement is obtained with increasing volume fraction.

5. REFERENCES

1. M. Nirmalkumar, V. Katti and S. V. Prabhu, Local heat transfer distribution on a smooth flat plate impinged by a slot jet, *International Journal of Heat and Mass Transfer* **54**, 727–738, 2011.
2. H. G. Lee, H. S. Yoon and M. Y. Ha, A numerical investigation on the fluid flow and heat transfer in the confined impinging slot jet in the low Reynolds number region for different channel heights, *International Journal of Heat and Mass Transfer* **51**, 4055–4068, 2008.
3. I. Dagtekin and H. F. Oztop, Heat transfer due to double laminar slot jets impingement onto an isothermal wall within one side closed long duct, *International Communications in Heat and Mass Transfer* **35**, 65–75, 2008.
4. X. Li, J. L. Gaddis and T. Wang, Multiple flow patterns and heat transfer in confined jet impingement, *International Journal of Heat and Fluid Flow* **26**, 746-754, 2005.
5. Y. Chen, C. Ma, M. Qin, Y. Li, Theoretical study on impingement heat transfer with single-phase free-surface slot jets, *International Journal of Heat and Mass Transfer* **48**, 3381-3386, 2005.
6. Z. Q. Lou, A. S. Mujumdar and C. Yap, Effects of geometric parameters on confined impinging jet heat transfer, *Applied Thermal Engineering* **25**, 2687–2697, 2005.
7. M. A. R. Sharif, A. Banerjee, Numerical analysis of heat transfer due to confined slot-jet impingement on a moving plate, *Applied Thermal Engineering* **29**, 532–540, 2009.
8. B. N. Hewakandamby, A numerical study of heat transfer performance of oscillatory impinging jets, *International Journal of Heat and Mass Transfer* **52**, 396–406, 2009.
9. H. F. Oztop, E. Abu-Nada, Numerical study of natural convection in partially heated rectangular enclosures called with nanofluids, *International Journal of Heat and Fluid Flow* **29**, 1326-1336, 2008.
10. O. Manca, P. Mesolella, S. Nardini, D. Ricci, Numerical study of a confined slot impinging jet with nanofluids, *Nanoscale Research Letters* **6**, 188, 2011.
11. Y. T. Yang, F. H. Lai, Numerical study of heat transfer enhancement with the use of nanofluids in radial flow cooling system, *International Journal of Heat and Mass Transfer* **53**, 5895–5904, 2010.
12. X. Wang, X. Xu, S. Choi, Thermal conductivity of nanoparticles fluid mixture, *Journal of Thermophysical Heat Transfer* **13**, 474-480, 1999.
13. R. Hamilton, O. Crosser, Thermal conductivity of heterogeneous two component systems, I & EC Fundamentals **3**, 187-191, 1962.
14. FLUENT Computational Fluid Dynamics Code Version 6.3.26, Fluent Inc.